Journal of Environmental Management 370 (2024) 123034

Contents lists available at ScienceDirect

Journal of Environmental Management

journal homepage: www.elsevier.com/locate/jenvman

Research article

Enhancing biochar production: A technical analysis of the combined influence of chemical activation (KOH and NaOH) and pyrolysis atmospheres (N_2/CO_2) on yields and properties of rice husk-derived biochar

Premchand Premchand [a,c], Francesca Demichelis [a,*], Camilla Galletti [a], David Chiaramonti [b], Samir Bensaid [a], Elsa Antunes [d], Debora Fino [a,**]

[a] Department of Applied Science and Technology, Politecnico di Torino, Corso Duca Degli Abruzzi 24, 10129, Turin, TO, Italy
[b] Department of Energy, Politecnico di Torino, Corso Duca Degli Abruzzi 24, 10129, Turin, TO, Italy
[c] Department of Science, Technology and Society, University School for Advanced Studies IUSS Pavia, 27100, Pavia, PV, Italy
[d] College of Science and Engineering, James Cook University, Townsville, Australia

ARTICLE INFO

Keywords:
Rice husk
Pyrolysis
CO_2 atmosphere
Chemical activation
Combined effect
Biochar properties

ABSTRACT

The production of biochar from biomass has received considerable interest due to its potential in environmental applications; however, optimizing biochar properties remains a major challenge. The objective of the present study was to investigate the synergistic effects of pyrolysis atmospheres (N_2 and CO_2) and chemical activation (pre- and post-pyrolysis) with NaOH and KOH on the properties of biochar useful for its environmental applications. In this study rice husk and biochar were impregnated with KOH and NaOH before and after pyrolysis, which was carried out at 600 °C under N_2 and CO_2 atmosphere. The pyrolytic yields (biochar, liquid and gas) and detailed characterization of biochar were performed. The results showed that pre-activation with both alkalis under a CO_2 atmosphere slightly decreased the biochar yield and carbon contents while increasing oxygen in biochars compared to N_2 atmosphere. Alkali pre-activation in the CO_2 atmosphere considerably increased the specific surface area and pore volume of biochars compared to the N_2 atmosphere, with KOH being more effective than NaOH. The maximum specific surface area (SSA) and pore volume (PV) of biochar obtained were 178.4 m^2/g and 0.60 cm^3/g for KOH activated biochar under CO_2, which were 3.2 times and 30 times higher than the untreated biochar. The post-activation of biochars with both alkalis resulted in moderate improvements in textural properties. Overall, chemical activation under CO_2 pyrolysis facilitated a higher level of chemical activation reactions leading to increased formation of oxygen functional groups and contributed to enhanced SSA and PV of the biochar useful for adsorption.

1. Introduction

The rising level of CO_2 emissions from anthropogenic activities as well as non-CO_2 greenhouse gas emissions from the agricultural sector (CH_4, N_2O), have led to a serious detrimental impact on our global ecosystem in terms of global warming, rising sea levels, heavy droughts, and heat waves (Lee et al., 2017; Lynch et al., 2021). Therefore, long-term effective mitigation strategies to address environmental challenges are urgently required. Among various strategies, biochar production from agricultural waste and its use for multiple applications, particularly environmental remediation, has been proposed as a potential environmental mitigation solution because of its unique physicochemical properties (Lehmann et al., 2021). Biochar is a carbon-rich stable solid that is produced when biomass is thermochemically converted in low-oxygen environments, typically via slow pyrolysis (Premchand et al., 2023b). The specific application of biochar is strongly dependent on its physicochemical properties such as surface area, porosity, functional groups, stability and mineral contents (Haghighi Mood et al., 2022), while the extent of these properties is heavily influenced by the type of feedstock and the production conditions like

* Corresponding author.
** Corresponding author.
E-mail addresses: francesca.demichelis@polito.it (F. Demichelis), debora.fino@polito.it (D. Fino).

https://doi.org/10.1016/j.jenvman.2024.123034
Received 15 July 2024; Received in revised form 21 September 2024; Accepted 20 October 2024
Available online 23 October 2024
0301-4797/© 2024 The Authors. Published by Elsevier Ltd. This is an open access article under the CC BY license (http://creativecommons.org/licenses/by/4.0/).

temperature, heating rate, and residence time (Ding and Liu, 2020).

Despite the wide range of beneficial properties of biochar produced directly from biomass via pyrolysis, its effectiveness in certain applications has been limited by its poor physicochemical properties, such as lower surface area and porosity, as well as fewer surface functional groups (Blenis et al., 2023; Shen and Fu, 2018). Therefore, these properties can further be modified to make them more appropriate for specific environmental applications such as adsorption (Panahi et al., 2020). Based on this, an extensive investigation has been conducted on various biochar modification techniques, including doping, ball milling, coating with carbonaceous materials, templating and activation before and after pyrolysis (Adeniyi et al., 2022; Bhuvanendran et al., 2021; Leng et al., 2021). Physical and chemical activation of biochar has been widely researched for engineering surface area and porosity, specifically for adsorption purposes, including physical activation via steam, carbon dioxide, and air (Sajjadi et al., 2019a), as well as chemical activation via acids, alkaline, and transition metals (Sajjadi et al., 2019b). Chemical activation is regarded to be more economically feasible than physical activation since it takes less processing time, reduces the activation temperature, and generates high-quality porous activated carbon (Patra et al., 2021). Among the chemical activating reagents, potassium hydroxide (KOH) and sodium hydroxide (NaOH) have frequently been reported to produce highly microporous activated biochars while also increasing the development of -OH functional groups on the biochar's surface (Haghighi Mood et al., 2022; Oginni et al., 2019; Stefanidou et al., 2021). Chen et al. (2020) pyrolyzed bamboo waste with KOH at 400–800 °C and discovered the formation of a significant number of new O-containing groups and a substantial rise in the surface and porosity. Similar trend of increasing surface area, porosity and oxygen functional groups have been reported by many studies (Bashir et al., 2018; Herath et al., 2021; Hu et al., 2022) using KOH as an activating agent. On the other hand, Lee et al. (2021) found that the specific surface area and pore volume of activated biochar were 106 times and 21 times greater than those of pristine biochar when they used NaOH as an activation agent during the pyrolysis of ground coffee residue for the adsorption of herbicides at 800 °C for 2 h and the trend is consistent with other reported studies of NaOH activation (Acemioğlu, 2022; Nguyen et al., 2021).

Chemical activation could be performed either before (pre-) or after (post-) pyrolysis by impregnating the precursor (biomass/biochar) with alkalis followed by thermal treatment (pyrolysis) (Sajjadi et al., 2019b). Compared to pre-activation, post-activation with alkalis yields higher surface area and porosity but less functional groups, therefore pre-activation is usually preferred because the post-activation process requires more energy and time (Leng et al., 2021).

Generally, alkaline hydroxides react with active oxygen species during pyrolysis to remove most oxygen groups, release free radicals, and create several vacancies. The OH^- ions from the alkali quickly fill these vacancies, forming new oxygen-containing groups in the biochar (Chen et al., 2020). Moreover, the structural modification of biochar is primarily caused by the oxidative and reductive processes induced by alkaline hydroxide, followed by thermal treatment. During this process, the graphitic layers separate and degrade, leaving the biochar with micro and mesopores (Sajjadi et al., 2019b).

Although it has been reported that activating biochar with NaOH and KOH before or after pyrolysis can significantly improve its physicochemical properties, nearly all the research has been conducted at high pyrolysis temperatures and in inert nitrogen atmospheres. These conditions could raise production costs and impede commercial production. However, recent studies (Premchand et al., 2023a, 2023b) have shown that substituting CO_2 for N_2 as the pyrolysis medium significantly alters the surface area, porosity, and functional groups of biochar, even at lower temperatures (600 °C). At higher pyrolysis temperatures (>600 °C), CO_2 promotes additional release of volatile matters and pores formation due to the oxidation of biochars, resulting in modified porosity (Kim et al., 2023). While at lower to medium temperatures (<600 °C), CO_2 is thought to improve porosity by reacting with volatile organic carbons (released from thermal degradation of the sample), which selectively trigger the morphological modification of biochar after volatile organic carbons are depleted (Cho et al., 2015; Premchand et al., 2023b). This suggests a promising direction for future research because using CO_2 could provide several advantages, including the ability to replace pure inert N_2, cost savings, improved biochar properties, lower environmental impact, and promotion of sustainable practices (Premchand et al., 2023a). Despite these developments, there is a substantial research gap regarding the use of CO_2 for biochar activation with KOH and NaOH during pyrolysis. To the best of authors' knowledge, no study has reported the synergistic effect of chemical activation and pyrolytic atmospheres (CO_2) on pyrolytic yields and biochar characteristics. Therefore, the present study aims to comparatively investigate the effects of pre- and post-pyrolysis activation with KOH and NaOH on pyrolysis performance (yields, gaseous compositions, biochar characteristics) at a moderate pyrolysis temperature of 600 °C in both N_2 and CO_2 atmospheres for rice husk (RH) feedstock. The objective was to enhance the textural properties and oxygen-containing functional groups of biochar, which are extremely useful for a variety of environmental applications such as pollutant removal from water, wastewater, and soils (Patra et al., 2021). RH was chosen for its abundant availability, low cost, and high carbon (42.99%) (Premchand et al., 2023b) and lignin contents (21.44%), as rice is grown in over 75 countries and produces approximately 80 million tons of RH per year worldwide (Shamsollahi and Partovinia, 2019), therefore choosing RH could mimic the applicability and relevance of our findings to real-world applications. Furthermore, because rice husk and other lignocellulosic biomasses have comparable structural composition (cellulose, hemicellulose, and lignin), this study may be applicable and adaptable to other lignocellulosic biomasses.

2. Materials and methods

2.1. Materials

The rice husk (RH) feedstock utilized for pyrolysis was supplied by Ecopack, Piobesi, Italy, with heterogeneous size distribution (8–10 mm). The RH was air dried with moisture content less than 7% and used without pre-treatment. The thermogravimetric analysis, elemental and proximate compositions of RH are provided in the Supplementary Materials (Fig. S1 and Table S2) and explained in detailed elsewhere (Premchand et al., 2023b). Briefly, RH contained 42.99% total carbon, 4.09% hydrogen, 1.79% nitrogen, 0.35% sulfur, and 50.79% oxygen, respectively. Furthermore, proximate analysis revealed 6.90% moisture content, 13.93% ash content, 72.11% volatile matter, and 7.06% fixed carbons.

The potassium hydroxide (≥85%, KOH basis, pellets) and sodium hydroxide (NaOH, reagent grade, ≥98%) were bought from Sigma Aldrich.

2.2. Biochar productions and activations

The schematic overview of the processes for biochar preparation, activation and analyses are depicted in Fig. 1.

2.2.1. Slow pyrolysis experiments

The details of the pyrolysis reactor setup, experimental and analytical procedure are described elsewhere (Premchand et al., 2023b). The slow pyrolysis experiments were carried out in a fixed-bed pyrolysis reactor, which was made up of a stainless-steel chamber with an electric heater and two thermocouples positioned at different levels within the reactor. Prior to heating, approximately 10 g of feedstock was manually added to the reactor and purged with N_2 or CO_2. The pyrolysis experiments were conducted at 600 °C, with a heating rate of 15 °C/min and residence time of 1h. These conditions were selected based on our

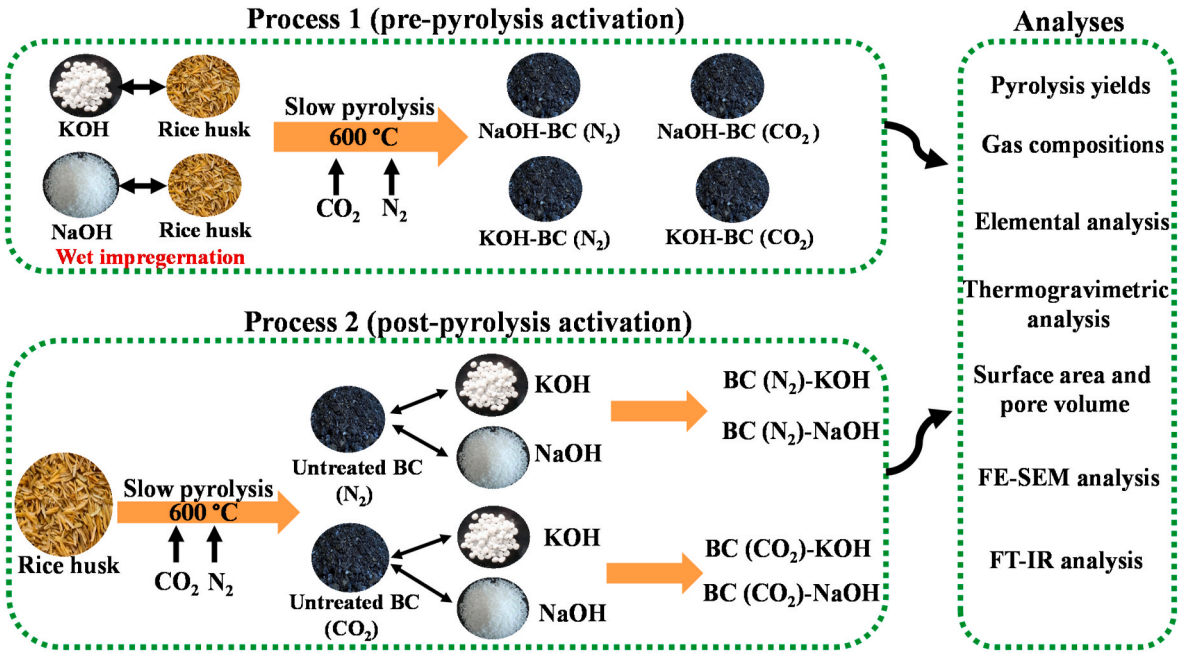

Fig. 1. Schematic overview of the process (methodologies).

previous study (Premchand et al., 2023b) which showed the optimal biochar characteristics (specific surface area and porosity). After pyrolysis, the reactor was allowed to cool before manually collecting the biochar.

2.2.2. Pre-pyrolysis activation of RH

For pre-pyrolysis activation, the RH feedstock was impregnated with KOH or NaOH in a weight-based impregnation ratio of 1:1. The sample was immersed in a 400 mL solution of KOH or NaOH and stirred continuously (200 RPM) in a 500 mL beaker on a magnetic stirrer heating plate for 24 h at room temperature. Following impregnation, the impregnated precursors were dried in an oven at 105 °C for 24 h, followed by a slow pyrolysis at 600 °C at a heating rate of 15 °C/min in N_2 or CO_2 atmospheres with a residence time of 1 h. After the pyrolysis process, the resultant biochar was washed several times with water to remove excess salts, filtered and oven dried for characterization analyses. The sequence of pre-pyrolysis activation process in depicted in Fig. 1.

2.2.3. Post-pyrolysis activation of biochar

For post-pyrolysis activation, first the biochar was produced via slow pyrolysis under N_2 or CO_2 atmospheres (600 °C; 15 °C/min; 1 h) and then biochar was impregnated with KOH or NaOH in a weight-based impregnation ratio of 1:1 using the procedure described in section 2.2.2.

In this study, the post-activation of biochar was carried out according to the wet activation method (Jamil et al., 2023) in which the biochar was impregnated in alkali solutions at room temperature for 24 h, filtered and oven dried (without being heated again). After drying impregnated biochar in an oven at 105 °C for 24 h, the biochar was washed several times with water to remove excess salts. This method was adopted to simplifies the process and considering environmental and economic factors (Zhou et al., 2019). The sequence of post-pyrolysis activation process in depicted in Fig. 1. Each experiment was performed three times (at least twice), and the mean values were reported with standard deviations.

2.3. Characterizations analyses

The composition of non-condensable pyrolytic gases was analyzed using a micro-GC (SRA Instruments) fitted with two columns: Molecular sieve 5A (argon carrier gas) and PoraPLOT U (helium carrier gas) and was calibrated for N_2, O_2, H_2, CO, CO_2, CH_4, C_2H_4, C_2H_6, and C_3.

The thermogravimetric analysis (TGA) of biochar was performed on a TGA analyzer (TGA/SDTA851e) by heating the samples from room temperature to 800 °C at a rate of 15 °C per minute. The CHN/S (carbon, hydrogen, nitrogen, and sulfur) analysis of feedstock/biochar was carried out with a CHNS analyzer (Elemental Cube, Germany) by combusting samples at 950 °C. The Bruker F-TIR Spectrophotometer Equinox 55 was utilized to analyze the surface functional groups of biochar in the 4000–400 cm^{-1} wavenumber range (ATR mode).

The textural analysis of biochar was performed on the Micromeritics TriStar II 3020 (surface area and porosity analyzer) with N_2 physisorption at −196 °C in liquid nitrogen. Before analysis, the samples were degassed in a vacuum for 2 h at 300 °C. Brunauer, Emmett, and Teller's (BET) method was used to calculate the specific surface area and total pore volume.

The morphology and elemental composition of the biochar were examined using a Zeiss Merlin Field Emission Scanning Electron Microscope (FESEM) equipped with an Oxford Instruments X-act EDS detector.

The biochar's pH was determined employing a digital pH meter (PH50 XS + DHS, GEASS S.r.L.), using biochar/water ratio of 1:20 (Premchand et al., 2023b).

Each analysis was performed three times (at least twice), and the mean values were reported with standard deviations.

3. Results and discussion

3.1. Pyrolysis product distribution

The biochar, liquid (oil and aqueous phase), and gas yields from the pyrolysis of RH (un-treated and alkaline impregnated) in N_2 and CO_2 atmospheres are displayed in Fig. 2a, and the pyrolytic gas compositions are shown in Fig. 2b. The labels RH (N_2) or RH (CO_2) indicate the pyrolysis experiment of untreated rice husk in a N_2 or CO_2 atmosphere, whereas RH + NaOH (N_2/CO_2) and RH + KOH (N_2/CO_2) represent the pyrolysis of NaOH and KOH impregnated rice husk in N_2 and CO_2 atmospheres, respectively.

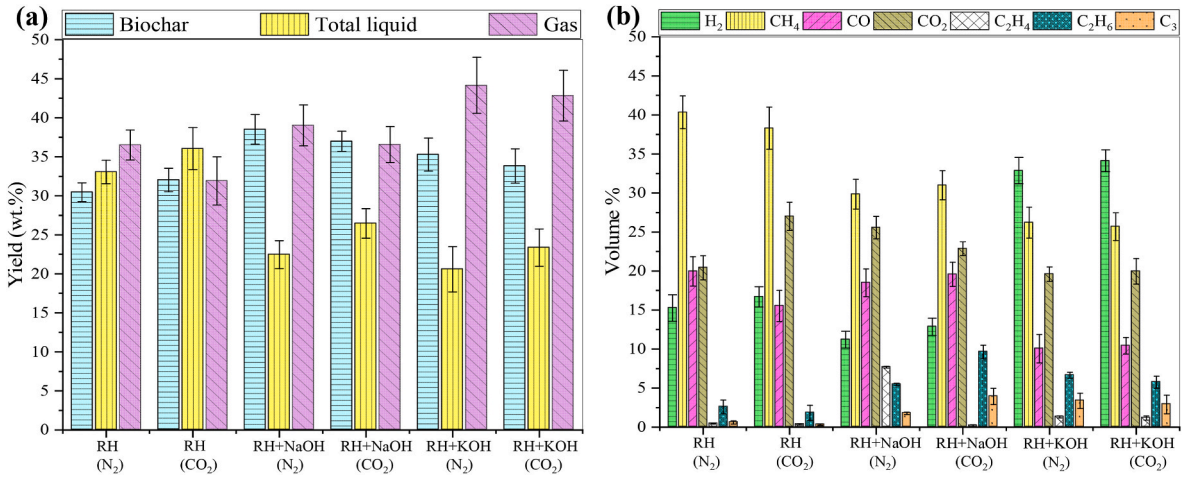

Fig. 2. Effect of NaOH and KOH impregnation and pyrolysis atmosphere (N_2 and CO_2) on: (a) the yield of biochar, liquid, and gas and (b) gaseous composition (integrated) from rice husk (RH) pyrolysis at 600 °C.

3.1.1. Pyrolysis of untreated RH under N_2 and CO_2 atmospheres

For untreated RH, CO_2 pyrolysis produced slightly more biochar (32.0%) and total liquid (36.1%), but significantly less gas (31.9%) than N_2 pyrolysis, which yielded 30.4% biochar, 33.0% total liquid, and 36.5% gas. The increase in biochar and liquid yield while decreases in gas yield by CO_2 atmosphere at lower to medium pyrolysis temperatures (300–600 °C) have been frequently reported in the literature for different feedstocks such as grape waste (Premchand et al., 2023b), rice straw (Biswas et al., 2018) and banana peel (Kwon et al., 2020). It may be because of the reactive nature of CO_2, the presence of CO_2 may have accelerated the breakdown of complex organic compounds into simpler molecules, some of which condensed into liquid products and some of which re-polymerized into solid products, resulting in a higher biochar and liquid yield while lowering the gas yield (Premchand et al., 2023a, 2023b). Among gaseous products, Overall, the volume % of CH_4 was found to be higher than that of CO_2 or CO in all experiments, which could be attributed to the gas collection stage. In the current study, the gas analyzed was only collected for 1 h of the pyrolysis stage (not the heating stage), which produced the relatively higher CH_4, excluding the capture of CO_2 and CO gases during the heating stage, which could have otherwise increased their proportions. Among atmosphere, the presence of CO_2 notably shifted the gas composition compared to the N_2 atmosphere, such that CO_2 pyrolysis produced more H_2 and CO_2, while less CH_4, CO, and other light hydrocarbons. The observed higher levels of H_2 and CO_2 while lower CO may be attributed to the partial effect of the water-gas shift reaction, in which water vapor reacted with CO (formed earlier from CO_2) and produced more H_2 and CO_2 while decreasing CO (Yoon et al., 2019).

3.1.2. Pyrolysis of pre-activated RH with NaOH under N_2 and CO_2 atmospheres

The pyrolytic yields and gas composition from RH impregnated with NaOH under N_2 and CO_2 atmospheres are depicted in Fig. 2a and b.

When compared to the pyrolysis of untreated RH under N_2 atmosphere, the yield of biochar and gas from RH impregnated with NaOH increased greatly from 30.5% to 38.5% (biochar) and 36.5%–39.0% (gas), while the total liquid yield decreased from 33.0% to 22.4%. The increased biochar and gas yields might be due to the catalytic properties of NaOH, which facilitated the formation of more stable char structures by removing volatile components such as CO_2 and H_2O via dehydration and decarboxylation reactions, while also promoting secondary cracking of volatiles, resulting in the formation of more gas products (Chen et al., 2021b; Guo et al., 2012). While the decreased liquid yield was likely due to the increased charring effect and secondary cracking of volatiles that would have otherwise contributed to the formation of liquid products.

Among gas compositions, compared to untreated RH, pyrolysis of RH impregnated with NaOH under N_2 atmosphere resulted in a lower concentration of H_2, CO, and CH_4 while increased concentrations of CO_2, C_2H_4, C_2H_6, and C_3 gases. Previous studies (Chen et al., 2021b) reported that the impregnation of biomass with NaOH increased the proportion of all gases, particularly H_2, because of the reaction of NaOH with carbon fragments in biomass, producing large amounts of H_2. Unlike, the decreased concentration of H_2, CO, and CH_4 and increased concentration CO_2, C_2H_4, C_2H_6, and C_3 gases observed in the current study indicate a shift in the chemical reactions taking place during pyrolysis. The NaOH may have promoted certain reactions that further converted these gases into higher hydrocarbons (Chen et al., 2008).

Among of pyrolysis atmosphere, compared to untreated RH, pyrolysis of RH impregnated with NaOH under CO_2 atmosphere also showed a similar trend (likewise N_2 atmosphere) of increasing biochar and gas yields and decreasing liquid yield as well similar trend in gas compositions. However, the pyrolytic yields and gas compositions differed when 2 atm were compared for RH impregnated with NaOH feedstock. For RH impregnated with NaOH, CO_2 atmosphere produced slightly less biochar (36.9%) and gas (36.5%), but significantly more liquid (26.47%) than in a N_2 atmosphere for the same feedstock. Among gas compositions, CO_2 atmosphere increased the concentrations of H_2, CH_4, CO, C_2H_6, and C_3, while decreased the concentration of CO_2 and C_2H_4 in comparison with N_2 atmosphere for RH impregnated with NaOH. Although no previous study directly reported the effect of CO_2 atmosphere on the pyrolysis of NaOH impregnated biomass, the findings in this study may be related to previous studies (Biswas et al., 2018; Premchand et al., 2023a, 2023b) on the effect of CO_2 atmosphere on pyrolysis of untreated biomass. The slight decrease in biochar yield under CO_2 could be attributed to the role of CO_2 in facilitating specific reactions that partially consumed the char. These could include the partial effect of the Boudouard reaction, in which char and CO_2 might have reacted to produce CO (Premchand et al., 2023a), as shown by slightly higher concentrations of H_2 and CO and lower concentration of CO_2 in gas compositions. However, this did not significantly increase the gas yield could be because some of the carbon in the gas may have condensed into liquid products which increased the total liquid yield (Biswas et al., 2018).

3.1.3. Pyrolysis of pre-activated RH with KOH under N_2 and CO_2 atmospheres

The pyrolytic yields and gas compositions from the pyrolysis of RH impregnated with KOH under N_2, and CO_2 atmospheres are shown in Fig. 2a and b.

In comparison to untreated RH, pyrolysis of RH impregnated with KOH under N_2 atmosphere significantly increased the biochar (from

30.4% to 35.2%) and gas yields (from 36.5% to 44.1%), while decreasing liquid yield (from 33.04% to 20.6%). Among gas compositions, the KOH impregnation drastically increased the concentration of H_2 from 15.2% to 32.9% while decreasing the concentrations of CH_4, CO, and CO_2. The findings were consistent with the previous studies (Chen et al., 2020; Hu et al., 2022). The increased biochar yield could be attributed to the catalytic effect of KOH, which may have accelerated the reactions that stabilized the char structure (Chen et al., 2020). KOH can effectively reduce volatile content while increasing char residue by promoting dehydration and decarboxylation reactions (Chen et al., 2020). On the other hand, increased gas yield and decreased liquid yield indicate that KOH promoted the fragmentation of larger molecular intermediates into smaller molecular gaseous products (Hu et al., 2022). Among gas composition, previous studies (Chen et al., 2020; Oginni et al., 2019) reported that the incorporation of KOH into biomass increased the relative concentrations of all gases being H_2 more significantly; however, in the current study, only H_2, C_2H_4, C_2H_6, and C_3 gases showed increased concentrations, while CH_4, CO, and CO_2 indicated decrease concentrations.

The observed differences could be attributed to a variety of factors, including pyrolysis conditions, biomass type, and KOH interaction with the gases. KOH may have favored certain catalytic reactions over others, altering the chemical equilibrium and reaction pathways during the pyrolysis process and thus influencing the composition of the final gas.

Examining the effect of the pyrolysis atmosphere, KOH also followed the same pattern as NaOH. of increasing biochar and gas yields while decreasing liquid yield compared to the pyrolysis of untreated RH. However, the pyrolytic yields and gas compositions were significantly different when 2 atm were compared for RH impregnated with KOH. Pyrolysis of RH impregnated with KOH under CO_2 atmosphere yielded slightly less biochar (33.8%) and gas (42.8%) but more liquid (23.3%) than under N_2 atmosphere for the same feedstock. Among gas compositions, the CO_2 atmosphere resulted in slightly higher concentrations of H_2, CO, and CO_2, while decreasing the concentrations of CH_4, C_2H_6, and C_3 in relative to N_2 atmosphere. Since no previous study has investigated the effect of CO_2 on the pyrolytic performance of KOH-impregnated biomass. However, the CO_2 atmosphere for the KOH-impregnated biomass followed the same pattern as for NaOH, therefore the possible reasons for KOH could be like NaOH, as discussed in the previous section (3.1.2) for NaOH.

3.2. Physicochemical characteristics of biochar

For the biochars, the label untreated BC (N_2/CO_2) indicates the biochar produced from untreated RH under N_2 or CO_2 atmosphere whereas NaOH-BC (N_2/CO_2) and KOH-BC (N_2/CO_2) represent pre-activated biochar produced from NaOH and KOH impregnated RH under N_2 or CO_2 atmosphere. The labels BC (N_2)-NaOH and BC (CO_2)-NaOH represent the post activated N_2 or CO_2 derived biochar with NaOH and label BC (N_2)-KOH or BC (CO_2)-KOH shows the post activated N_2 or CO_2 derived biochar with KOH.

3.2.1. Elemental analysis and pH

3.2.1.1. Pre-pyrolysis activated biochar. The elemental analysis, pH and metal (EDS) analysis of untreated and pre-pyrolysis activated biochars are listed in Tables 1 and 2 and the representative EDS spectra are presented in Supplementary Materials (Figs. S2–S6).

For untreated biochars, CO_2 atmosphere slightly increased the carbon content in biochar from 72.0% to 74.0% while decreased the hydrogen content from 2.3 to 2.1%, and oxygen content from 23.9% to

Table 2
EDS analysis (metal composition in weight % balanced with C and O) of untreated biochars, pre-pyrolysis activated biochars and post-pyrolysis activated biochars derived from rice husk (RH) at pyrolysis temperature of 600 °C under N_2 and CO_2 atmospheres.

Sample	Si (%)	Ca (%)	Mg (%)	K (%)	Na (%)	S (%)	P (%)
Untreated BC (N_2)	9.86 ± 0.32	0.13 ± 0.02	0.18 ± 0.01	0.63 ± 0.23	N/D	N/D	N/D
Untreated BC (CO_2)	10.63 ± 1.05	0.19 ± 0.08	0.14 ± 0.05	0.63 ± 0.13	N/D	N/D	N/D
NaOH-BC (N_2)	2.21 ± 0.92	0.42 ± 0.09	0.12 ± 0.01	0.17 ± 0.08	4.46 ± 1.33	N/D	N/D
NaOH-BC (CO_2)	1.44 ± 0.98	0.06 ± 0	0.09 ± 0.01	0.29 ± 0.51	5.54 ± 1.11	N/D	N/D
KOH-BC (N_2)	0.11 ± 0.10	1.06 ± 0.06	N/D	7.03 ± 2.58	N/D	N/D	0.08 ± 0.01
KOH-BC (CO_2)	0.88 ± 0.21	N/D	0.10 ± 0.01	9.95 ± 2.30	0.08 ± 0	N/D	N/D
BC (N_2)-NaOH	1.67 ± 1.12	0.58 ± 0.24	0.68 ± 0.21	0.52 ± 0.32	1.99 ± 0.24	0.04 ± 0	0.61 ± 0.09
BC (CO_2)-NaOH	1.61 ± 0.38	0.33 ± 0.17	N/D	0.34 ± 0.06	N/D	0.62 ± 0.25	N/D
BC (N_2)-KOH	3.95 ± 0.60	0.61 ± 0.22	0.12 ± 0.01	2.01 ± 0.14	N/D	N/D	N/D
BC (CO_2)-KOH	3.02 ± 0.20	0.49 ± 0.02	0.15 ± 0.06	1.14 ± 0.10	N/D	0.27 ± 0.10	N/D

Table 1
Elemental analysis (weight percentages) and pH of untreated biochars, pre-pyrolysis activated biochars and post-pyrolysis activated biochars derived from rice husk (RH) at pyrolysis temperature of 600 °C under N_2 and CO_2 atmospheres.

Sample	Carbon (%)	Hydrogen (%)	Nitrogen (%)	Sulfur (%)	Oxygen[a] (%)	pH
Without treatment						
Untreated BC (N_2)	72.00 ± 2.14	2.30 ± 0.11	1.68 ± 0.07	0.12 ± 0.001	23.90 ± 2.14	8.84 ± 0.02
Untreated BC (CO_2)	74.09 ± 2.08	2.09 ± 0.13	1.68 ± 0.18	0.11 ± 0.002	22.03 ± 2.09	9.68 ± 0.01
Pre-pyrolysis activated						
NaOH-BC (N_2)	60.91 ± 3.2	2.26 ± 0.19	0.67 ± 0.19	0.06 ± 0.002	36.10 ± 3.21	8.25 ± 0.05
NaOH-BC (CO_2)	62.14 ± 2.62	2.34 ± 0.30	0.52 ± 0.04	0.08 ± 0.002	34.92 ± 2.64	8.95 ± 0.04
KOH-BC (N_2)	65.08 ± 1.54	2.29 ± 0.08	1.13 ± 0.03	0.05 ± 0.001	31.45 ± 1.54	8.51 ± 0.02
KOH-BC (CO_2)	63.11 ± 1.05	2.17 ± 0.02	0.57 ± 0.16	0.06 ± 0.001	34.09 ± 1.06	8.99 ± 0.03
Post-pyrolysis activated						
BC (N_2)-NaOH	67.33 ± 2.13	4.67 ± 0.07	1.43 ± 0.26	0.02 ± 0.001	26.56 ± 2.15	7.99 ± 0.01
BC (CO_2)-NaOH	66.21 ± 2.87	2.15 ± 0.08	1.55 ± 0.05	0.02 ± 0.001	30.07 ± 2.87	8.11 ± 0.04
BC (N_2)-KOH	67.51 ± 3.61	1.74 ± 0.37	1.34 ± 0.14	0.04 ± 0.002	29.37 ± 3.63	8.01 ± 0.06
BC (CO_2)-KOH	71.08 ± 2.96	2.64 ± 0.33	1.51 ± 0.23	0.02 ± 0.002	24.75 ± 2.99	8.15 ± 0.01

[a] By difference.

22.0%, which were consistent with previous studies (Biswas et al., 2018; Premchand et al., 2023b). Furthermore, the pH of CO_2 biochar was 1.1 times higher than that of N_2 biochar, which could be attributed to the higher ash content as reported in our previous study (Premchand et al., 2023b). Meal analysis revealed that RH biochars were primarily composed of silicon (Si) (9.86–10.63%), followed by calcium (Ca), potassium (K), and magnesium (Mg) with negligible difference among the pyrolysis atmospheres.

When RH was impregnated with NaOH and pyrolyzed under N_2 atmosphere, the carbon content in pre-pyrolysis activated biochar significantly decreased from 72.0% to 60.9%, the hydrogen content decreased from 2.3% to 2.2%, the nitrogen content decreased from 1.7% to 0.7%, and the oxygen content increased from 23.9% to 36.1%, which were consistent with previous studies (Chen et al., 2021b). The decreased carbon and hydrogen content could be attributed to the increased reactivity of biochar caused by NaOH during pyrolysis, which may have increased the formation of volatile carbon and hydrogen compounds that released carbon and hydrogen as gases or liquid products (Haghighi Mood et al., 2022). Conversely, the significant rise in oxygen content observed in biochar can be attributed to the reaction between NaOH and biomass, which potentially introduced oxygen-containing functional groups such as hydroxyls and carboxylates into the char structure (Chen et al., 2021b).

Among atmospheres, likewise N_2, CO_2 atmosphere also increased oxygen content while decreasing all other elements in activated biochar in comparison with untreated biochar. However, elemental compositions of activated biochars varied slightly between 2 atm for the same feedstock (RH impregnated with NaOH). For example, compared to the N_2 atmosphere, activated biochar produced from CO_2 retained more carbon (62.1%) and hydrogen (2.3%), while less oxygen (34.9%) and the reason could be the more carbonization effect aided by the CO_2 as previously mentioned.

On the other hand, pre-pyrolysis activation with KOH followed the same trend as NaOH, but to a different extent. For example, compared to untreated biochar, KOH under N_2 atmosphere decreased carbon content from 72.0% to 65.0%, hydrogen content from 2.30% to 2.29%, and increased oxygen content from 23.9% to 31.4%. The reaction between KOH and carbon fragments could be the primary cause of reduced carbon, whereas the dehydrogenation reaction might be responsible for the decrease in hydrogen content (Chen et al., 2020). Moreover, the increase in oxygen content may be attributed to the reaction between KOH and biomass, introducing additional oxygen-containing functional groups.

Among atmospheres, CO_2 had the opposite effect on elemental analysis of KOH activated biochar as it did on NaOH activated biochar in comparison with N_2 atmosphere. For example, compared to the N_2 atmosphere, KOH activated biochar produced in the CO_2 atmosphere contained less carbon (63.1%), less hydrogen (2.17%), and more oxygen (34.09%) compared to N_2 atmosphere with the same feedstock. These findings demonstrate that the CO_2 atmosphere influenced the elemental composition of activated biochars with KOH and NaOH differently, possibly due to the different catalytic effects of NaOH and KOH on biomass pyrolysis.

Upon examining metal compositions, it was found that the silicon content in pre-pyrolysis activated biochars was significantly reduced from 10.6 % to 0.1 % when activated with alkali. This could be attributed to the leaching or dissolving action of alkalis, which may have broken down silica and converted it into soluble silicates that were washed away during the post-pyrolysis washing process (Motlagh et al., 2021). However, the biochar samples contained significant proportion of K (9.9%) and Na (5.5%), which could be either due to leftover inorganic salts or as part of the carbon structure as stable salts, e.g., K_2CO_3, Na_2CO_3 that remained even after pyrolysis and washing (Chen et al., 2020, 2021b).

Regarding the pH of the biochars, as stated in section 2.2.2, prior to analysis, the resultant biochars were washed several times with distilled water to remove excess salts which ultimately reduced the pH compared to untreated biochars. However, all the biochars were still alkaline with pH ranging from 8.2 to 8.9, with KOH and CO_2 higher than NaOH and N_2 in the atmosphere.

3.2.1.2. Post-pyrolysis activated biochars. The elemental analysis of post-pyrolysis activated biochars with NaOH and KOH showed significant variations in comparison with untreated biochars (Table 1), however to a lesser extent than pre-pyrolysis activated biochars and was obviously because of not exposing to higher temperatures (Zhao et al., 2022). For example, when N_2 derived biochar was post activated with NaOH or KOH, the carbon content noticeably decreased from 72.0% to 67.3% (NaOH) and 51.7% (KOH), while oxygen content increased form from 23.9% to 26.6% (NaOH) and 45.2% (KOH). Along with a slight decrease in hydrogen, nitrogen, and sulfur contents was also observed with few exceptions. A similar trend was observed for CO_2 derived biochar but with more profound effect. The decrease in carbon contents might be either because of the high alkalinity of NaOH or KOH which eroded the biochar (Chen et al., 2021a) or alkali activation facilitated the removal of carbon as soluble organic compounds during the washing process (Li et al., 2022).

On the other hand, the significant increase in oxygen contents by NaOH and KOH post activation for both biochars (N_2 and CO_2) indicates that the NaOH and KOH may have added oxygen-containing groups to the biochar structure or stabilized existing oxygen functionalities, making the biochar more hydrophilic.

In terms of metal composition (Table 2), likewise pre-activation, post-activation of biochars with both alkalis also reduced the Si contents to minimum 1.6% which could be attributed to alkalis' leaching or dissolving action, as previously mentioned. The post-activated biochars, on the other hand, contained minimal proportions of K and Na (less than 2% when compared to pre-activated), indicating that washing biochars several times with water successfully removed the leftover inorganic salts. Furthermore, post-activated biochars had a slightly lower pH than untreated and pre-pyrolysis activated biochars, but they remained alkaline (7.9–8.1).

3.2.2. Thermogravimetric analysis

The weight loss behaviors against temperature (TGA) of untreated biochars, pre-pyrolysis activated, and post-pyrolysis activated biochars are given in Fig. 3.

Examining the thermal behaviors of untreated biochars produced under N_2 and CO_2 atmospheres (Fig. 3a), until about 400 °C, both biochars showed identical patterns with negligible weight losses, indicating that the primary volatile components were already removed during the pyrolysis process. As the temperature rose from 400 to 800 °C, both biochars began to lose weight in this range, with N_2 biochar consistently losing slightly more weight (7% total loss) than CO_2 biochar (5% total loss). According to literature studies (Kim et al., 2021; Premchand et al., 2023b), the CO_2 atmosphere increases the fixed carbons and ashes in biochar by removing more volatile matter from biomass than the N_2 atmosphere, possibly explaining the slightly more thermally stable biochar observed in the current study.

3.2.2.1. Pre-pyrolysis activated biochars. The effect of NaOH and KOH pre-activation and pyrolysis atmospheres on the weight loss behavior of activated biochars is shown in Fig. 3b.

The TGA curves of NaOH pre-activated biochars differed significantly from those of untreated biochars in terms of weight loss pattern, resulting in greater weight loss under both pyrolysis atmospheres. For example, untreated biochars lost only 7% (N_2 atmosphere) and 5% (CO_2 atmosphere) of their total weight at 800 °C, whereas NaOH pre-activated biochars lost 25% (N_2 atmosphere) and 15% (CO_2 atmosphere) of their total weight. Furthermore, the onset of weight loss for the NaOH-treated biochars started much earlier than for the untreated biochar which might be attributed to activation energy distribution.

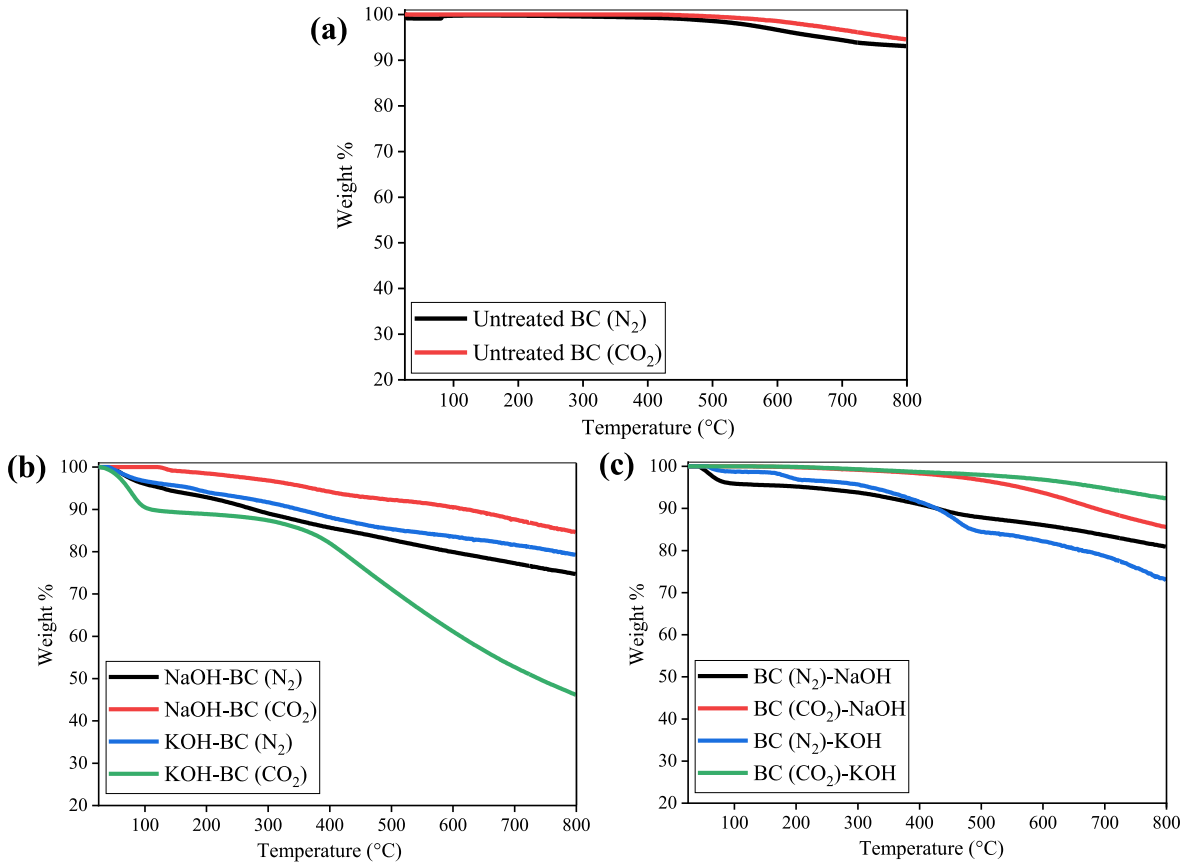

Fig. 3. TGA (weight loss behavior) curves of different biochars: (a) untreated biochars under N_2 and CO_2 atmosphere, (b) pre-pyrolysis activated biochars with NaOH and KOH, and (c) post-pyrolysis activated biochars with NaOH and KOH.

On the other hand, when comparing the TGA curves of KOH pre-activated biochars to untreated biochars, likewise NaOH, KOH pre-activation also significantly changed the weight loss pattern, resulting in higher weight loss under both pyrolytic atmospheres. For example, at 800 °C, KOH pre-activated biochars lost 20% (N_2 atmosphere) and 53% (CO_2 atmosphere) of total weight compared to 7% and 5% for untreated biochars. Overall, regardless of the pyrolysis atmosphere, pre-activation with alkalis (NaOH and KOH) significantly reduced the thermal stability of activated biochars when compared to untreated biochars. These findings can be attributed to the various changes to biochar caused by alkali activation, such as improved volatile matter removal, increased porosity, and chemical modification of the carbon structure (Tayibi et al., 2019).

The KOH/NaOH activation resulted in an increase in oxygen and a decrease in carbon content, which primarily occurred in surface functional groups that are more susceptible to desorption and thermal degradation, resulting in lower thermal stability (Jedynak and Charmas, 2024).

In terms of pyrolysis atmospheres, CO_2 had varying effects on the TGA of NaOH and KOH pre-activated biochars. For NaOH, the CO_2 atmosphere caused less weight loss (15%) than the N_2 atmosphere (25%); however, for KOH, the CO_2 atmosphere caused greater weight loss (53%) than the N_2 atmosphere (20%). This suggests a significant difference between the reaction pathways facilitated by KOH and NaOH in a CO_2 atmosphere. Under CO_2, KOH may have catalyzed the formation of less stable structures, leading to a faster degradation rate, whereas with NaOH it promoted the formation of more stable cross-linked structures, improving thermal stability. A similar contrasting effect was also observed in the elemental analysis thus indicating that the type of activation agent (NaOH and KOH) had a greater impact on the thermal stability of the biochar than did the pyrolysis atmosphere (N_2 and CO_2) or total carbon contents. On the other hand, the relationship between carbon and thermal stability appeared to be influenced by the nature of carbon produced by the different alkali activation than the total carbons, such as aromaticity and functional groups (Xu et al., 2021).

3.2.2.2. Post-pyrolysis activated biochars. The TGA curves of post-pyrolysis activated biochars with NaOH and KOH are given in Fig. 3c. The weight loss of untreated biochar derived from N_2 pyrolysis was only 7%; however, this weight loss increased to 19% when biochar was post-activated with NaOH and 27% when post-treated with KOH. Conversely, the 5% weight loss of untreated biochar from CO_2 pyrolysis became 15% with NaOH post activation and 7% with KOH post activation.

These findings show that, in terms of thermal stability, post-activation of CO_2 derived biochars with KOH and NaOH produced more stable biochars than N_2 derived biochars post-treated with KOH and NaOH. This might have resulted from CO_2 pyrolysis, which produced more stable carbon structures (Premchand et al., 2023a) that were less reactive to alkali treatments. However, among alkalis, varying effects were observed between KOH and NaOH, most likely due to their different basicity, which could result in different interactions with the carbon matrix (Sajjadi et al., 2019b).

3.2.3. Specific surface area and pore volume analysis

The specific surface area (SSA) and pore volume (PV) of untreated, pre-pyrolysis activated, and post-pyrolysis activated biochars are listed in Table 3.

Examining the untreated biochars, it was observed that the CO_2 atmosphere produced biochar with a higher SSA (141.0 m^2/g) and PV (0.08 cm^3/g) than the N_2 atmosphere, which produced biochar with a 55.7 m^2/g SSA and 0.02 cm^3/g PV. It has been widely reported that the

Table 3
Specific surface area and pore volumes of untreated, pre-pyrolysis activated, and post-pyrolysis activated biochars derived from rice husk (RH) at pyrolysis temperature of 600 °C under N_2 and CO_2 atmospheres.

	Specific surface area (m^2/g)	Pore volume (cm^3/g)
Without treatment		
Untreated BC (N_2)	55.7 ± 1.02	0.018 ± 0.001
Untreated BC (CO_2)	141.0 ± 1.03	0.084 ± 0.002
Pre-pyrolysis activated		
NaOH-BC (N_2)	102.3 ± 0.95	0.268 ± 0.001
NaOH-BC (CO_2)	123.0 ± 0.99	0.255 ± 0.003
KOH-BC (N_2)	117.6 ± 1.01	0.341 ± 0.004
KOH-BC (CO_2)	178.4 ± 0.85	0.598 ± 0.004
Post-pyrolysis activated		
BC (N_2)-NaOH	68.7 ± 1.04	0.127 ± 0.003
BC (CO_2)-NaOH	107.6 ± 1.01	0.101 ± 0.001
BC (N_2)-KOH	99.0 ± 0.98	0.197 ± 0.003
BC (CO_2)-KOH	152.0 ± 0.69	0.311 ± 0.002

CO_2 atmosphere significantly improves the textural properties of biochar due to its gasification and increased thermal cracking effects during pyrolysis (Komiyama and Uemura, 2022; Kwon et al., 2020; Lee et al., 2017). The literature studies provided a more detailed explanation of the possible effects of CO_2 (Lee et al., 2017; Premchand et al., 2023a, 2023b).

3.2.3.1. Pre-pyrolysis activated biochars. Pre-pyrolysis activation of biochars with KOH/NaOH under different pyrolytic atmospheres (N_2/CO_2) resulted in significant textural changes in activated biochars.

Compared to untreated biochar, pre-activation with NaOH under N_2 atmosphere significantly increased the SSA from 55.7 to 102.3 m^2/g (1.8 times), and PV from 0.02 to 0.27 cm^3/g (13.5 times). Moreover, CO_2 atmosphere further increased the SSA to 123.0 m^2/g (2.2 times), and PV to 0.26 cm^3/g (13 times) in comparison with untreated biochar. This might be because NaOH as a chemical activating agent (Haghighi Mood et al., 2022), may have reacted with the carbonaceous matrix in biochar, causing the formation of new pores and the expansion of existing ones. This reaction usually removes volatile components from the biochar matrix, resulting in a more porous structure (Chen et al., 2021b; Nguyen et al., 2021). The addition of CO_2 may have amplified the activation effects initiated by NaOH, resulting in a more prominent development of the biochar's internal pore structure and surface area because CO_2 is well known to alter the pathways of biomass thermal degradation, favoring the formation or retention of more porous structures during pyrolysis (Lee et al., 2017; Premchand et al., 2023a). Therefore, the synergistic effect of NaOH as a chemical activating agent and CO_2 as a physical activating agent both contributed to increased SSA and PV of the biochar.

On the other hand, KOH exhibited a similar pattern of increasing SSA and PV, but with a more profound effect than NaOH. Compared to untreated biochar, pre-activation with KOH under N_2 atmosphere increased the SSA from 55.7 to 117.6 m^2/g (2.1 times), and PV from 0.02 to 0.34 cm^3/g (17 times). The CO_2 atmosphere further increased the SSA to 178.4 m^2/g (3.2 times), and PV to 0.60 cm^3/g (30 times) in comparison with untreated biochar. The possible reasons for this could be the same as for NaOH (discussed earlier); however, the significant differences observed between the two alkalis might be because KOH is a stronger basic agent than NaOH, so it may have interacted more effectively with the carbonaceous material in biochar, resulting in the enhanced formation of new pores by intensifying the chemical activation process (Patra et al., 2021; Sajjadi et al., 2019b). Moreover, the combined synergistic effect of KOH and CO_2 further intensified the activation reactions which led to higher SSA and PV in biochar.

Overall, the findings showed that KOH was more effective than NaOH at increasing the SSA and PV of biochar, and the CO_2 atmosphere further greatly enhanced these effects compared to the N_2 atmosphere.

3.2.3.2. Post-pyrolysis activated biochars. Post-pyrolysis activation of biochars with NaOH and KOH also showed a moderate effect on the textural properties of the activated biochars, as shown in Table 3.

When biochar produced under N_2 atmosphere was post-activated with NaOH, the SSA of the biochar increased from 55.7 to 68.7 m^2/g, while PV increased from 0.02 to 0.13 cm^3/g. When the same biochar was post-activated with KOH, its SSA increased to 99.0 m^2/g and PV to 0.19 cm^3/g. Most of the previous studies (Seo et al., 2021; Sun et al., 2015) reported that post-activation of biochar with alkalis without subjecting to higher temperatures reduced the surface area and porosity due to the blockage of the pores by alkali crystals. However, the observed improvements in the textural properties of post-activated biochars in the current study can be attributed to several factors. First, alkalis can dissolve ash and mineral matter in biochar, which usually clog pores or take up space within the pore structure. Therefore, alkali treatments and the subsequent washing procedure may have removed these materials and enhanced the porosity (Wang et al., 2022). Second, the swelling action of alkalis or surface chemistry modification may also contribute to the increased porosity.

On the other hand, the post-activation of biochar produced from CO_2 pyrolysis also followed a similar trend of increasing surface area and porosity, except for NaOH post-treatment, which decreased the SSA of biochar from 141.0 to 107.6 m^2/g. The observed decrease in SSA shows that NaOH may have caused structural collapse or pore blockage in CO_2 biochar. This could be caused by contact of NaOH with certain carbon structures produced during CO_2 pyrolysis, which may be more vulnerable to pores collapsing.

3.2.4. FE-SEM analysis

The morphologies of untreated, pre-pyrolysis activated, and post-pyrolysis activated biochars under N_2 and CO_2 atmospheres are presented in Fig. 4.

Looking at the morphologies of untreated biochars (Fig. 4a and b), N_2 biochar showed a denser and smoother structure with fewer visible pores and a more closed surface. In contrast, the CO_2 biochar (Fig. 4b) showed a much more porous and rough structure, with several visible pores and a more open texture, which reflected the increased SSA and PV discussed in section 3.2.3 and was consistent with the previous studies (Lee et al., 2017; Premchand et al., 2023b). As mentioned earlier, CO_2 might change the kinetics and chemical reactions of pyrolysis and promote the growth of mesopores and micropores by speeding up the breakdown of organic compounds (Premchand et al., 2023b).

3.2.4.1. Pre-pyrolysis activated biochars. Examining the effect of NaOH pre-activation on biochar's morphology, compared to untreated biochar, the NaOH activation significantly altered the biochar's morphologies under both N_2 and CO_2 atmospheres. NaOH pre-activated biochar under N_2 atmosphere (Fig. 4c) showed certain structural changes, with a much rougher texture and higher density of pores compared to untreated biochar (Fig. 4a). These observations were consistent with the previous study on the pre-pyrolysis activation of coffee residue with NaOH (Lee et al., 2021). Moreover, the structure of activated biochar exhibited even greater porosity and an uneven pore structure with larger irregularly shaped pores and in a CO_2 atmosphere (Fig. 4d). These findings were aligned with the changes in textural characteristics as discussed in section 3.2.3. The NaOH was likely to create new pores and widen the existing pores by eroding the organic components (Chen et al., 2021b; Sajjadi et al., 2019b), while CO_2 further enhanced the activation effect in comparison with N_2 atmosphere.

On the other hand, KOH pre-activation also revealed notable visual morphological differences when compared to untreated biochars. As shown in Fig. 4e, KOH pre-activation under N_2 atmosphere introduced lot of new visible micro pores on biochar surface compared to untreated biochar. This demonstrated the successful activation of biochar with KOH, and similar observations were reported in previous studies of pre-

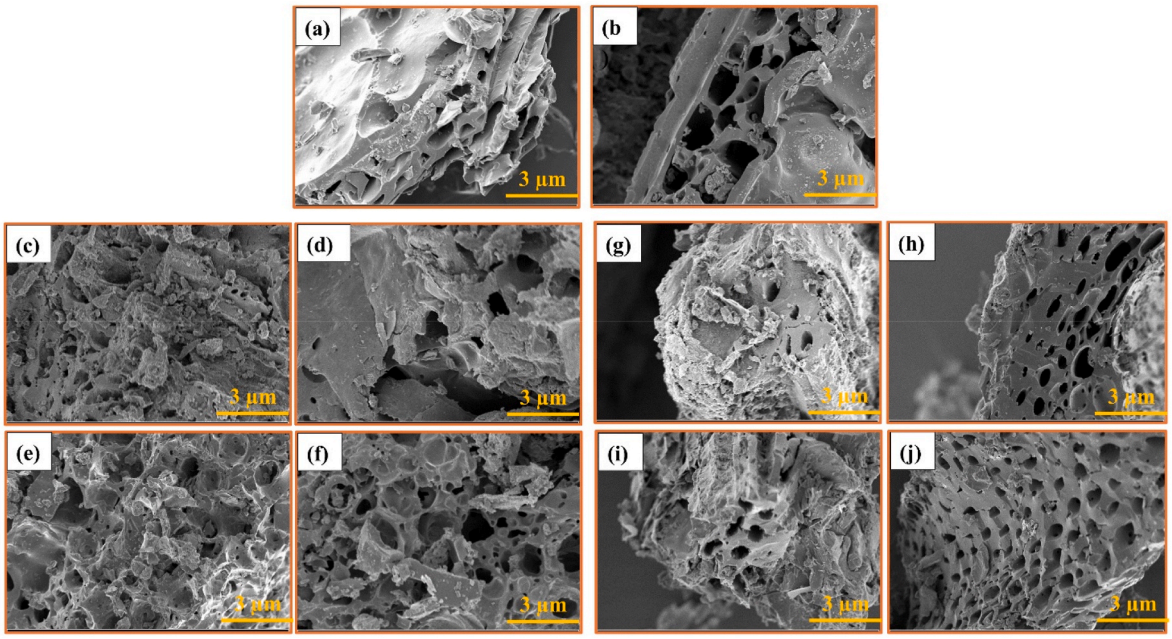

Fig. 4. FE-SEM images of biochars at 3 µm scale with 5.00 K X magnification: (a) untreated BC (N_2); (b) untreated BC (CO_2); (c) NaOH-BC (N_2); (d) NaOH-BC (CO_2); (e) KOH-BC (N_2); (f) KOH-BC (CO_2); (g) BC (N_2)-NaOH; (h) BC (CO_2)-NaOH; (i) BC (N_2)-KOH and (j) BC (CO_2)-KOH.

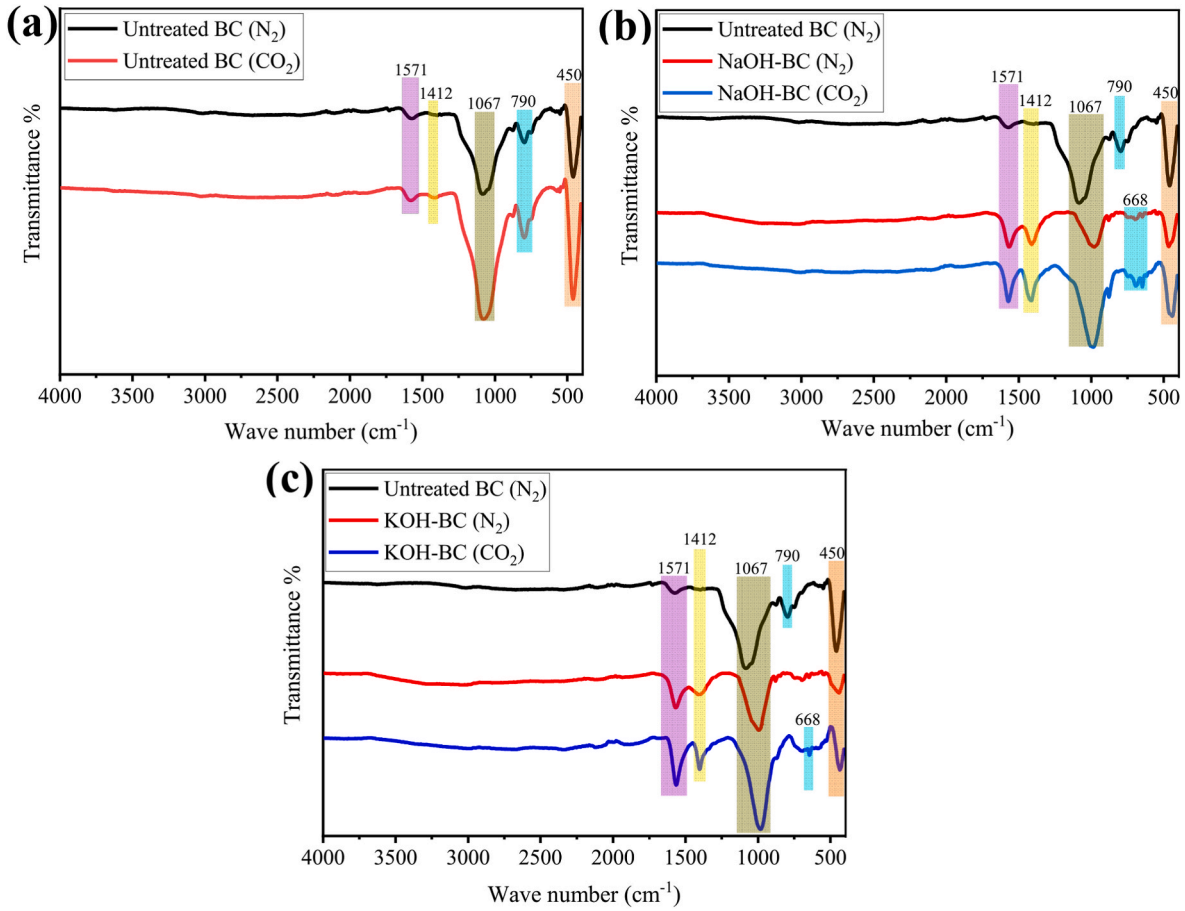

Fig. 5. FT-IR spectra of biochars: (a) pristine biochars from un-treated RH under N_2 and CO_2 atmosphere; (b) biochars produced from NaOH pre-treated RH under N_2 and CO_2 atmosphere; and (c) biochars produced from KOH pre-treated RH under N_2 and CO_2 atmosphere.

pyrolysis biochar activation with KOH (Li et al., 2022; Oginni et al., 2019). During pyrolysis, the combined effects of KOH's chemical activation, oxidative etching, and pore widening significantly improve the porosity of biochar, which ultimately increase the SSA, PV and more micro and mesopores (Chen et al., 2020, 2021b). Furthermore, the CO_2 atmosphere revealed greater porosity, with a more pronounced porous structure and more visible micro and macro pores (Fig. 4f), which could be attributed to the synergistic effect of KOH and CO_2, which may have intensified certain chemical reactions, resulting in increased porosity.

3.2.4.2. Post-pyrolysis activated biochars. The morphologies of post-pyrolysis activated biochars with NaOH and KOH also showed distinct visual differences from the untreated biochars.

When N_2 biochar was post-activated with NaOH (Fig. 4g), the biochar surface became rougher and slightly more porous with many micro and nano pores than the untreated biochar (Fig. 4a), which clearly showed the few visible larger pores and in line with the previous study observation (Seo et al., 2021). In contrast, KOH post-activated biochar (Fig. 4i) exhibited a noticeably more porous structure, with a rough texture and many visible macro pores. This effect of enhanced structural changes by post activation could result from the alkalis dissolving the ash and mineral matter in the biochar, which blocked the pore structure (Wang et al., 2022).

On the other hand, when CO_2 biochar was post-treated with NaOH (Fig. 4h), the surface seemed slightly smoother than the untreated biochar (Fig. 4b), however with some pore structures became less defined. In contrast, the KOH post-activation of CO_2 biochar (Fig. 4j) clearly showed rougher texture, with visibly larger and more irregular pores

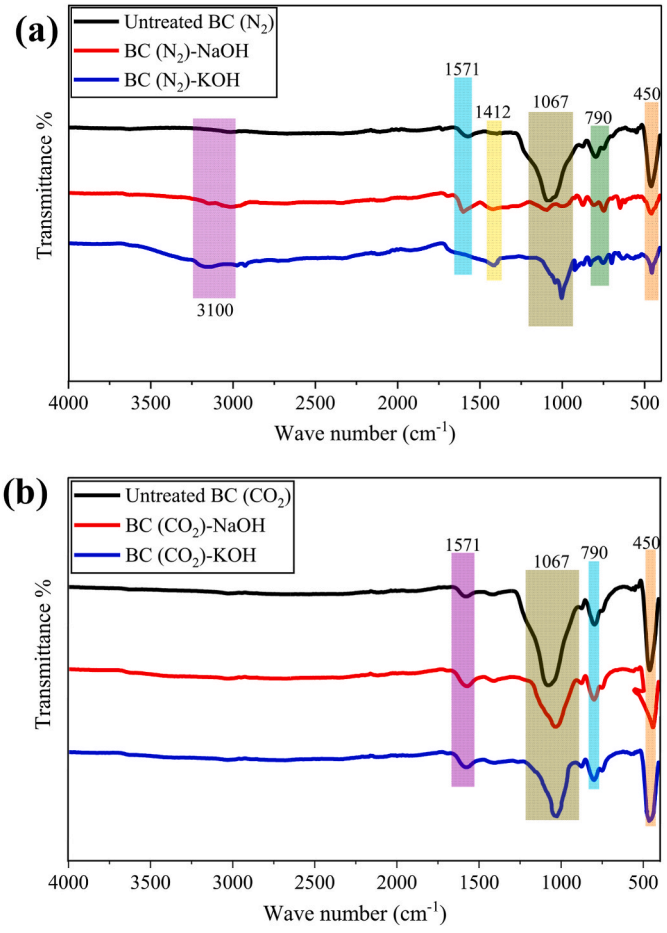

Fig. 6. FT-IR spectra of biochars: (a) N_2 biochars post-treated with NaOH and KOH, and (b) CO_2 biochars post-treated with NaOH and KOH.

than the untreated biochar. These findings reflected the observed changes in SSA and PV of the post-activated biochars in section 3.2.3.2.

3.2.5. FT-IR analysis

The FT-IR spectra of various biochars (untreated, pre-pyrolysis and post-pyrolysis activated biochar) are presented in Figs. 5 and 6.

The FT-IR spectra of untreated biochars produced in N_2 and CO_2 atmospheres (Fig. 5a) revealed that both biochars contained certain surface functional groups. The peak at 1571 cm^{-1} represented C=O stretching vibrations indicating various carbonyl groups (Premchand et al., 2023b), while the peak at 1412 cm^{-1} reflected O-H stretching vibrations in carboxylic acids (Hu et al., 2022; Komiyama and Uemura, 2022). A large and sharp peak at 1067 cm^{-1} corresponded to Si-O-Si stretching, indicating the presence of silicates related to the mineral composition of Si present in the rice husk (Morales et al., 2021; Wei et al., 2017). Furthermore, the peak at 790 cm^{-1} attributed to C-H bending in aromatic compounds, indicating the presence of substituted aromatic rings (Qureshi et al., 2021) and the peak at 450 cm^{-1} may reflected Si-H bending, suggesting the presence of silicon hydrides or related silicon-containing functional groups in the biochar (Wei et al., 2017). When comparing the 2 atm, it appeared that both biochars contained all the same functional groups; however, biochar produced from the CO_2 atmosphere exhibited different intensities of some peaks than biochar produced from the N_2 atmosphere. For instance, the slightly higher intensity of the O-H peak at 1412 cm^{-1} in the CO_2 biochar suggested a slightly more presence of -OH groups, whereas the more prominent and sharper peak at 1067 cm^{-1} in the CO_2 biochar suggested a higher content of silicates in CO_2 biochar. Furthermore, the slight increase in intensity of C-H peak at 790 cm^{-1} reflected a higher presence of aliphatic C-H bonds in CO_2 -derived biochar.

3.2.5.1. Pre-pyrolysis activated biochars. Looking at the effect of NaOH pre-activation on functional groups of activated biochars, as shown in Fig. 5b, compared to untreated biochar, NaOH pre-activation resulted in significant changes in functional groups in both N_2 and CO_2 atmospheres.

Compared to untreated biochar, NaOH pre-activated biochar showed higher peak intensities at 1571 cm^{-1} and 1412 cm^{-1}, representing the C=O and O-H groups, respectively. This suggests that NaOH facilitated certain reactions that enhanced the carboxylic and hydroxyl groups on the surface of the biochar (Lee et al., 2021). The initial peak intensity at 1067 cm^{-1} was greatly reduced and shifted to 991 cm^{-1}, most likely because of interactions with NaOH changed the silica structures.

Furthermore, the original peak at 790 cm^{-1} peak (C-H vibrations) completely disappeared whereas a tiny new peak at 668 cm^{-1} appeared, most likely indicating carbonate formations (Hu et al., 2022). On the other hand, when the NaOH biochar was pre-activated under CO_2 atmosphere, the peak intensities at 1571 and 1412 cm^{-1} were more pronounced than in N_2, indicated the higher presence of carboxylic and hydroxyl groups. The peak intensity at 1067 cm^{-1} remained same but shifted to 991 cm^{-1}, indicating a preserved silica network in CO_2 atmosphere. Furthermore, CO_2 biochar also showed a new peak at 668 cm^{-1}, like the N_2 atmosphere, but with higher intensity, indicating significant formation of carbonate structures.

On the other hand, KOH preactivated biochar under N_2 and CO_2 atmospheres (Fig. 5c) showed a similar effect to NaOH, but to a different extent. Under N_2 atmosphere, the KOH pre-activated biochar showed higher peak intensities of both peaks at 1571 cm^{-1} and 1412 cm^{-1} (C=O and O-H groups) compared to untreated biochar indicating increasing containing functional groups (Chen et al., 2021b). Moreover, the peak at 1067 cm^{-1} shifted to a lower wave number (around 994 cm^{-1}), while the peak at 790 cm^{-1} vanished completely. Furthermore, the intensity of the peak at around 450 cm^{-1} was significantly reduced, indicating that silicate minerals were being removed by KOH.

When the biochar was pre-activated with KOH in a CO_2 atmosphere,

the peak intensities of both peaks at 1571 cm^{-1} and 1412 cm^{-1} significantly increased compared to all the biochars investigated. This suggests that the synergistic effect of strong chemical activator (KOH) and CO_2 facilitates a higher level of certain processes, leading to more extensive formation of these oxygen-containing functional groups. The findings were consistent with the elemental analysis where the treatment of KOH/NaOH increased the oxygen content in biochars.

3.2.5.2. Post-pyrolysis activated biochars. Examining the effect of NaOH/KOH post-activation on functional groups of activated biochars, as shown in Fig. 6, compared to untreated biochars derived from N_2 or CO_2 pyrolysis, the NaOH and KOH post-treatment led to noticeable changes in surface functional groups.

When N_2 biochar was post-treated with NaOH, a new broad peak around 3100 cm^{-1} (O-H stretching vibrations) appeared suggesting the increased hydroxyl groups on the biochar surface (Wang et al., 2022). The intensity of the carbonyl peak at 1571 cm^{-1} showed a slight increase in C=O functionalities. Moreover, post-activation with NaOH significantly reduced the peak intensities at 1067 cm^{-1} and 450 cm^{-1}, indicating the removal of silica-based compounds.

On the other hand, KOH post-activation of N_2 biochar also showed similar effect on functional groups as NaOH, with increased intensities of hydroxyl and carbonyl functionalities and decreased peak intensities of silica functionalities Fig. 6a.

Conversely, post-activation of CO_2 biochars with NaOH and KOH (Fig. 6b) had significantly different and negligible effects on surface functional groups than on N_2 biochars particularly in removing the silica structures. Unlike N_2 biochar, CO_2 biochar post-treated with NaOH and KOH, retained all the silica related peaks at 1067 and 450 cm^{-1} with slight increased peak intensity of C=O functionalities at 1571 cm^{-1}.

4. Conclusions

This study examined the effects of pre-pyrolysis and post-pyrolysis chemical activation with alkalis (NaOH and KOH) and pyrolysis atmosphere (N_2 and CO_2) on the pyrolytic performance and detailed physicochemical properties of rice husk biochar produced at 600 °C. The results showed that, compared to N_2 atmosphere, alkali pre-activations under CO_2 atmosphere significantly increased biochar's surface area, pore volume, and oxygen functional groups, with KOH being more effective than NaOH due to its high basicity. Thermogravimetric analysis revealed that the type of activation agent (NaOH or KOH) had a greater influence on the thermal stability of the biochar than the pyrolysis atmosphere. Overall, for the pre-activation, the addition of CO_2 significantly enhanced the activation effects initiated by alkaline hydroxides, resulting in a more apparent development of the biochar's internal pore structure and surface area by promoting the formation or retention of more porous structures during pyrolysis. On the other hand, post-activation of N_2 and CO_2 pyrolysis derived biochars showed moderate improvements in the textural properties of biochars, which may be due to alkali treatments and the subsequent washing procedure removed the ash materials, which enhanced the porosity.

Thus, using waste CO_2 (rather than pure N_2) in the pyrolysis process for chemical activation of biochar could provide numerous benefits, including increased porosity and oxygen functional groups of biochar, which are highly useful for a variety of environmental applications such as pollutant removal from water, wastewater, and soils, as well as cost savings and reduced greenhouse gas emissions.

CRediT authorship contribution statement

Premchand Premchand: Writing – original draft, Visualization, Validation, Investigation, Data curation. **Francesca Demichelis:** Writing – original draft, Validation, Methodology, Formal analysis, Data curation, Conceptualization. **Camilla Galletti:** Writing – review & editing, Formal analysis. **David Chiaramonti:** Writing – review & editing, Supervision. **Samir Bensaid:** Writing – review & editing, Supervision. **Elsa Antunes:** Writing – review & editing, Supervision. **Debora Fino:** Writing – review & editing, Supervision, Resources, Project administration, Funding acquisition.

Declaration of competing interest

The authors declare that they have no known competing financial interests or personal relationships that could have appeared to influence the work reported in this paper.

Acknowledgments

This article and related research were carried out as part of the Italian inter-university PhD program in sustainable development and climate change (https://www.phd-sdc.it/).

Appendix A. Supplementary data

Supplementary data to this article can be found online at https://doi.org/10.1016/j.jenvman.2024.123034.

Data availability

Data will be made available on request.

References

Acemioğlu, B., 2022. Removal of a reactive dye using NaOH-activated biochar prepared from peanut shell by pyrolysis process. Int. J. Coal Prep. Util. 42 (3), 671–693. https://doi.org/10.1080/19392699.2019.1644326.

Adeniyi, A.G., Abdulkareem, S.A., Iwuozor, K.O., Ogunniyi, S., Abdulkareem, M.T., Emenike, E.C., Sagboye, P.A., 2022. Effect of salt impregnation on the properties of orange albedo biochar. Clean. Chem. Eng. 3, 100059. https://doi.org/10.1016/j.clce.2022.100059.

Bashir, S., Zhu, J., Fu, Q., Hu, H., 2018. Comparing the adsorption mechanism of Cd by rice straw pristine and KOH-modified biochar. Environ. Sci. Pollut. Res. 25, 11875–11883. https://doi.org/10.1007/s11356-018-1292-z.

Bhuvanendran, N., Ravichandran, S., Kandasamy, S., Zhang, W., Xu, Q., Khotseng, L., Maiyalagan, T., Su, H., 2021. Spindle-shaped CeO_2/biochar carbon with oxygen-vacancy as an effective and highly durable electrocatalyst for oxygen reduction reaction. Int. J. Hydrogen Energy 46 (2), 2128–2142. https://doi.org/10.1016/j.ijhydene.2020.10.115.

Biswas, B., Singh, R., Kumar, J., Singh, R., Gupta, P., Krishna, B.B., Bhaskar, T., 2018. Pyrolysis behavior of rice straw under carbon dioxide for production of bio-oil. Renew. Energy 129, 686–694. https://doi.org/10.1016/j.renene.2017.04.048.

Blenis, N., Hue, N., Maaz, T.M., Kantar, M., 2023. Biochar production, modification, and its uses in soil remediation: a review. Sustainability 15 (4), 3442. https://doi.org/10.3390/su15043442.

Chen, H., Yang, X., Liu, Y., Lin, X., Wang, J., Zhang, Z., Li, N., Li, Y., Zhang, Y., 2021a. KOH modification effectively enhances the Cd and Pb adsorption performance of N-enriched biochar derived from waste chicken feathers. Waste Manag. 130, 82–92. https://doi.org/10.1016/j.wasman.2021.05.015.

Chen, M.-q., Wang, J., Zhang, M.-x., Chen, M.-g., Zhu, X.-f., Min, F.-f., Tan, Z.-c., 2008. Catalytic effects of eight inorganic additives on pyrolysis of pine wood sawdust by microwave heating. J. Anal. Appl. Pyrolysis 82 (1), 145–150. https://doi.org/10.1016/j.jaap.2008.03.001.

Chen, W., Gong, M., Li, K., Xia, M., Chen, Z., Xiao, H., Fang, Y., Chen, Y., Yang, H., Chen, H., 2020. Insight into KOH activation mechanism during biomass pyrolysis: chemical reactions between O-containing groups and KOH. Appl. Energy 278, 115730. https://doi.org/10.1016/j.apenergy.2020.115730.

Chen, W., Li, K., Chen, Z., Xia, M., Chen, Y., Yang, H., Chen, X., Chen, H., 2021b. A new insight into chemical reactions between biomass and alkaline additives during pyrolysis process. Proc. Combust. Inst. 38 (3), 3881–3890. https://doi.org/10.1016/j.proci.2020.06.023.

Cho, D.-W., Cho, S.-H., Song, H., Kwon, E.E., 2015. Carbon dioxide assisted sustainability enhancement of pyrolysis of waste biomass: a case study with spent coffee ground. Bioresour. Technol. 189, 1–6. https://doi.org/10.1016/j.biortech.2015.04.002.

Ding, S., Liu, Y., 2020. Adsorption of CO_2 from flue gas by novel seaweed-based KOH-activated porous biochars. Fuel 260, 116382. https://doi.org/10.1016/j.fuel.2019.116382.

Guo, D.-l., Wu, S.-b., Liu, B., Yin, X.-l., Yang, Q., 2012. Catalytic effects of NaOH and Na_2CO_3 additives on alkali lignin pyrolysis and gasification. Appl. Energy 95, 22–30. https://doi.org/10.1016/j.apenergy.2012.01.042.

Haghighi Mood, S., Pelaez-Samaniego, M.R., Garcia-Perez, M., 2022. Perspectives of engineered biochar for environmental applications: a review. Energy Fuels 36 (15), 7940–7986. https://doi.org/10.1021/acs.energyfuels.2c01201.

Herath, A., Layne, C.A., Perez, F., Hassan, E.B., Pittman Jr, C.U., Mlsna, T.E., 2021. KOH-activated high surface area Douglas Fir biochar for adsorbing aqueous Cr (VI), Pb (II) and Cd (II). Chemosphere 269, 128409. https://doi.org/10.1016/j.chemosphere.2020.128409.

Hu, M., Ye, Z., Zhang, Q., Xue, Q., Li, Z., Wang, J., Pan, Z., 2022. Towards understanding the chemical reactions between KOH and oxygen-containing groups during KOH-catalyzed pyrolysis of biomass. Energy 245, 123286. https://doi.org/10.1016/j.energy.2022.123286.

Jamil, U., Zeeshan, M., Khan, S.R., Saeed, S., 2023. Synthesis and two-step KOH based activation of porous biochar of wheat straw and waste tire for adsorptive exclusion of chromium (VI) from aqueous solution; thermodynamic and regeneration study. J. Water Process Eng. 53, 103892. https://doi.org/10.1016/j.jwpe.2023.103892.

Jedynak, K., Charmas, B., 2024. Adsorption properties of biochars obtained by KOH activation. Adsorption 30 (2), 167–183. https://doi.org/10.1007/s10450-023-00399-7.

Kim, H.-B., Kim, J.-G., Kim, T., Alessi, D.S., Baek, K., 2021. Interaction of biochar stability and abiotic aging: influences of pyrolysis reaction medium and temperature. Chem. Eng. J. 411, 128441. https://doi.org/10.1016/j.cej.2021.128441.

Kim, H., Kim, S., Lee, J., Kim, M., Kwon, D., Jung, S., 2023. Pyrolysis of rice husk using CO_2 for enhanced energy production and soil amendment. Energy Environ. 34 (4), 873–885. https://doi.org/10.1177/0958305X221079422.

Komiyama, M., Uemura, Y., 2022. A comparative study of oil palm fronds torrefaction under flue gas and nitrogen atmospheres. J. Oil Palm Res. 35 (1), 75–85. https://doi.org/10.21894/jopr.2022.0027.

Kwon, D., Lee, S.S., Jung, S., Park, Y.-K., Tsang, Y.F., Kwon, E.E., 2020. CO_2 to fuel via pyrolysis of banana peel. Chem. Eng. J. 392, 123774. https://doi.org/10.1016/j.cej.2019.123774.

Lee, J., Yang, X., Cho, S.-H., Kim, J.-K., Lee, S.S., Tsang, D.C., Ok, Y.S., Kwon, E.E., 2017. Pyrolysis process of agricultural waste using CO_2 for waste management, energy recovery, and biochar fabrication. Appl. Energy 185, 214–222. https://doi.org/10.1016/j.apenergy.2016.10.092.

Lee, Y.-G., Shin, J., Kwak, J., Kim, S., Son, C., Cho, K.H., Chon, K., 2021. Effects of NaOH activation on adsorptive removal of herbicides by biochars prepared from ground coffee residues. Energies 14 (5), 1297. https://doi.org/10.3390/en14051297.

Lehmann, J., Cowie, A., Masiello, C.A., Kammann, C., Woolf, D., Amonette, J.E., Cayuela, M.L., Camps-Arbestain, M., Whitman, T., 2021. Biochar in climate change mitigation. Nat. Geosci. 14 (12), 883–892. https://doi.org/10.1038/s41561-021-00852-8.

Leng, L., Xiong, Q., Yang, L., Li, H., Zhou, Y., Zhang, W., Jiang, S., Li, H., Huang, H., 2021. An overview on engineering the surface area and porosity of biochar. Sci. Total Environ. 763, 144204. https://doi.org/10.1016/j.scitotenv.2020.144204.

Li, K., Zhang, D., Niu, X., Guo, H., Yu, Y., Tang, Z., Lin, Z., Fu, M., 2022. Insights into CO_2 adsorption on KOH-activated biochars derived from the mixed sewage sludge and pine sawdust. Sci. Total Environ. 826, 154133. https://doi.org/10.1016/j.scitotenv.2022.154133.

Lynch, J., Cain, M., Frame, D., Pierrehumbert, R., 2021. Agriculture's contribution to climate change and role in mitigation is distinct from predominantly fossil CO_2-emitting sectors. Front. Sustain. Food Syst. 4, 518039. https://doi.org/10.3389/fsufs.2020.518039.

Morales, L.F., Herrera, K., López, J.E., Saldarriaga, J.F., 2021. Use of biochar from rice husk pyrolysis: assessment of reactivity in lime pastes. Heliyon 7 (11), e08423. https://doi.org/10.1016/j.heliyon.2021.e08423.

Motlagh, E.K., Sharifian, S., Asasian-Kolur, N., 2021. Alkaline activating agents for activation of rice husk biochar and simultaneous bio-silica extraction. Bioresour. Technol. Rep. 16, 100853. https://doi.org/10.1016/j.biteb.2021.100853.

Nguyen, V.-T., Nguyen, T.-B., Huang, C., Chen, C.-W., Bui, X.-T., Dong, C.-D., 2021. Alkaline modified biochar derived from spent coffee ground for removal of tetracycline from aqueous solutions. J. Water Process Eng. 40, 101908. https://doi.org/10.1016/j.jwpe.2020.101908.

Oginni, O., Singh, K., Oporto, G., Dawson-Andoh, B., McDonald, L., Sabolsky, E., 2019. Influence of one-step and two-step KOH activation on activated carbon characteristics. Bioresour. Technol. Rep. 7, 100266. https://doi.org/10.1016/j.biteb.2019.100266.

Panahi, H.K.S., Dehhaghi, M., Ok, Y.S., Nizami, A.-S., Khoshnevisan, B., Mussatto, S.I., Aghbashlo, M., Tabatabaei, M., Lam, S.S., 2020. A comprehensive review of engineered biochar: production, characteristics, and environmental applications. J. Clean. Prod. 270, 122462. https://doi.org/10.1016/j.jclepro.2020.122462.

Patra, B.R., Mukherjee, A., Nanda, S., Dalai, A.K., 2021. Biochar production, activation and adsorptive applications: a review. Environ. Chem. Lett. 19, 2237–2259. https://doi.org/10.1007/s10311-020-01165-9.

Premchand, P., Demichelis, F., Chiaramonti, D., Bensaid, S., Fino, D., 2023a. Biochar production from slow pyrolysis of biomass under CO_2 atmosphere: a review on the effect of CO_2 medium on biochar production, characterisation, and environmental applications. J. Environ. Chem. Eng. 110009. https://doi.org/10.1016/j.jece.2023.110009.

Premchand, P., Demichelis, F., Chiaramonti, D., Bensaid, S., Fino, D., 2023b. Study on the effects of carbon dioxide atmosphere on the production of biochar derived from slow pyrolysis of organic agro-urban waste. Waste Manag. 172, 308–319. https://doi.org/10.1016/j.wasman.2023.10.035.

Qureshi, S.S., Premchand, Javed, M., Saeed, S., Abro, R., Mazari, S.A., Mubarak, N.M., Siddiqui, M.T.H., Baloch, H.A., Nizamuddin, S., 2021. Hydrothermal carbonization of oil palm trunk via taguchi method. Kor. J. Chem. Eng. 38, 797–806. https://doi.org/10.1007/s11814-021-0753-0.

Sajjadi, B., Chen, W.-Y., Egiebor, N.O., 2019a. A comprehensive review on physical activation of biochar for energy and environmental applications. Rev. Chem. Eng. 35 (6), 735–776. https://doi.org/10.1515/revce-2017-0113.

Sajjadi, B., Zubatiuk, T., Leszczynska, D., Leszczynski, J., Chen, W.Y., 2019b. Chemical activation of biochar for energy and environmental applications: a comprehensive review. Rev. Chem. Eng. 35 (7), 777–815. https://doi.org/10.1515/revce-2018-0003.

Seo, D.-C., Guo, R., Lee, D.-H., 2021. Performance of alkaline impregnated biochar derived from rice hull for hydrogen sulfide removal from gas. Environ. Eng. Res. 26 (6). https://doi.org/10.4491/eer.2020.452.

Shamsollahi, Z., Partovinia, A., 2019. Recent advances on pollutants removal by rice husk as a bio-based adsorbent: a critical review. J. Environ. Manag. 246, 314–323. https://doi.org/10.1016/j.jenvman.2019.05.145.

Shen, Y., Fu, Y., 2018. KOH-activated rice husk char via CO_2 pyrolysis for phenol adsorption. Mater. Today Energy 9, 397–405. https://doi.org/10.1016/j.mtener.2018.07.005.

Stefanidou, M., Kamperidou, V., Konstantinidis, A., Koltsou, P., Papadopoulos, S., 2021. Use of Posidonia oceanica fibres in lime mortars. Construct. Build. Mater. 298, 123881. https://doi.org/10.1016/j.conbuildmat.2021.123881.

Sun, K., Tang, J., Gong, Y., Zhang, H., 2015. Characterization of potassium hydroxide (KOH) modified hydrochars from different feedstocks for enhanced removal of heavy metals from water. Environ. Sci. Pollut. Res. 22, 16640–16651. https://doi.org/10.1007/s11356-015-4849-0.

Tayibi, S., Monlau, F., Fayoud, N.-e., Oukarroum, A., Zeroual, Y., Hannache, H., Barakat, A., 2019. One-pot activation and pyrolysis of Moroccan Gelidium sesquipedale red macroalgae residue: production of an efficient adsorbent biochar. Biochar 1 (4), 401–412. https://doi.org/10.1007/s42773-019-00033-2.

Wang, H., Wang, X., Teng, H., Xu, J., Sheng, L., 2022. Purification mechanism of city tail water by constructed wetland substrate with NaOH-modified corn straw biochar. Ecotoxicol. Environ. Saf. 238, 113597. https://doi.org/10.1016/j.ecoenv.2022.113597.

Wei, L., Huang, Y., Li, Y., Huang, L., Mar, N.N., Huang, Q., Liu, Z., 2017. Biochar characteristics produced from rice husks and their sorption properties for the acetanilide herbicide metolachlor. Environ. Sci. Pollut. Res. 24, 4552–4561. https://doi.org/10.1007/s11356-016-8192-x.

Xu, Z., He, M., Xu, X., Cao, X., Tsang, D.C., 2021. Impacts of different activation processes on the carbon stability of biochar for oxidation resistance. Bioresour. Technol. 338, 125555. https://doi.org/10.1016/j.biortech.2021.125555.

Yoon, K., Lee, S.S., Ok, Y.S., Kwon, E.E., Song, H., 2019. Enhancement of syngas for H_2 production via catalytic pyrolysis of orange peel using CO_2 and bauxite residue. Appl. Energy 254, 113803. https://doi.org/10.1016/j.apenergy.2019.113803.

Zhao, J., Ye, Z.-L., Pan, X., Cai, G., Wang, J., 2022. Screening the functions of modified rice straw biochar for adsorbing manganese from drinking water. RSC Adv. 12 (24), 15222–15230. https://doi.org/10.1039/D2RA01720B.

Zhou, N., Wang, Y., Yao, D., Li, S., Tang, J., Shen, D., Zhu, X., Huang, L., Zhong, M.-e., Zhou, Z., 2019. Novel wet pyrolysis providing simultaneous conversion and activation to produce surface-functionalized biochars for cadmium remediation. J. Clean. Prod. 221, 63–72. https://doi.org/10.1016/j.jclepro.2019.02.176.